Petrophysical and seismic signature of a heavy oil sand reservoir: Manitou Lake, Saskatchewan

Maria F. Quijada and Robert R. Stewart

ABSTRACT

A suite of well logs from the Manitou Lake heavy oil field in Saskatchewan was analyzed to study the effect of lithology and saturating fluid on density and P- and S-wave velocities in the sand reservoirs. The Vp values do not change significantly from shale to sand, but the shear-wave velocity increases significantly from 800 to 1300 m/s. A Vp/Vs value lower than 2.15 indicate sand reservoirs. Within the target zone, densities lower than 2250 kg/m^3 indicate sands. Modeling with the log response equation shows improvement in density estimations in comparison to using Gardner's relation. PP and PS synthetics show an opposite seismic signature at the top of the reservoir, seen as a trough on the PP section and as a peak in the PS section, making registration between the two sections more complex. Bright spots are expected on the PS section where sand is present. Post-stack impedance inversion shows promise for delineating the sand channels at the Colony top.

INTRODUCTION

The prediction of elastic properties such as density, P- and S-wave velocities, as well as their relations to rock properties such as lithology, porosity or fluid content, is critically important in reservoir characterization. This analysis also constitutes a crucial step for different applications such as seismic modelling, amplitude versus offset (AVO) variations.

Seismic velocities are affected by mineralogy, porosity, pore geometry and fluid, effective stress, cementation, and fractures. Shear waves are slower than compressional waves, polarized and cannot propagate through fluids, making converted-wave exploration useful for fluid and lithology discrimination, imaging structure through gas clouds and fracture detection by analysis of shear wave splitting, among other applications (Garotta et al., 2002). The bulk density of a rock is a function of porosity, hydrocarbon fluid type, water saturation, and mineral composition. Crossplots between rock properties and lithology and pore fluid indicate that density often provides the best differentiation between hydrocarbon reservoirs and other rock/fluid types (Van Koughnet et al., 2003), making accurate density estimates significant for reservoir characterization. Density can also be an important acoustic indicator of the presence of shale, making it an important parameter in oil sands or heavy oil developments where accurate density estimates are necessary to determine the location of shales in the reservoirs, which may interfere with the steaming or recovery process (Gray et al., 2006).

In the following sections several aspects of the estimation of elastic properties are evaluated. Well log data is analysed to better define the correlation between elastic and rock properties in the area of study. Different empirical and rock physics approaches are used to estimate elastic properties from different logs, and to define local parameters.

Finally, elastic parameters are estimated from seismic data by post-stack inversion of the PP volume.

AREA OF STUDY

The Manitou Lake oilfield is located in west central Saskatchewan, approximately 50 km southeast of the city of Lloydminster (Figure 1). Production in this field comes mainly from the Colony and Sparky B members of the Cretaceous Mannville group. The Lloydminster heavy oil accumulation is the southern extension of a discontinuous trend of Lower Cretaceous bitumen and heavy oil deposits, extending from Athabasca through Cold Lake to Lloydminster (Orr et al., 1977). Heavy oil gravity in the Lloyminster pools ranges from 10 to 25 °API. The Sparky pool in the Manitou Lake field was discovered in 1970 and there are currently 159 wells producing heavy oil with a gravity of 15.1°API within an area of 1441 Ha. The mean depth of the Sparky reservoir is 605 m with a net pay of 4.05 m. Core data shows that the average maximum permeability is 573 mD, porosity is 0.16 and water saturation is 0.3.

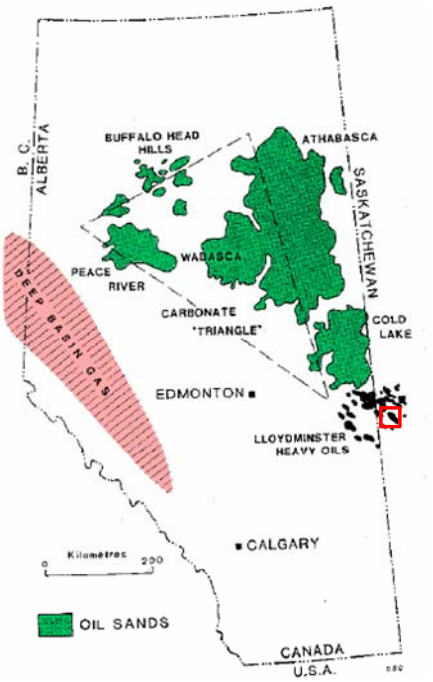

FIG. 1. Location of the Manitou Lake oilfield, Saskatchewan (From Stanton, 2004).

GEOLOGIC SETTING

The geology of the Lloydminster heavy oil region is quite complex from depositional, structural and economical perspectives, due to extreme lateral facies variations and features associated with salt dissolution (Putnam, 1982). Figure 2 shows the stratigraphic column for west-central Saskatchewan. Most of the sediments in the area were deposited during the Cretaceous, and the top of the Mannville Group marks a clear separation between the predominant sands in Mannville and the overlying marine shales of the Colorado and Belly River Groups. The Mannville Group lies unconformably on Paleozoic strata, and its sedimentary pattern consists of an interplay of marine, estuarine

and fluviatile agents acting in a setting controlled by paleo-topographic relief and eustatic and tectonic changes in relative sea-levels (Christopher, 1997). The thickness of Mannville sediments deposited in the area was controlled to a large degree by the relief on the pre-Cretaceous unconformity (Putnam, 1982).

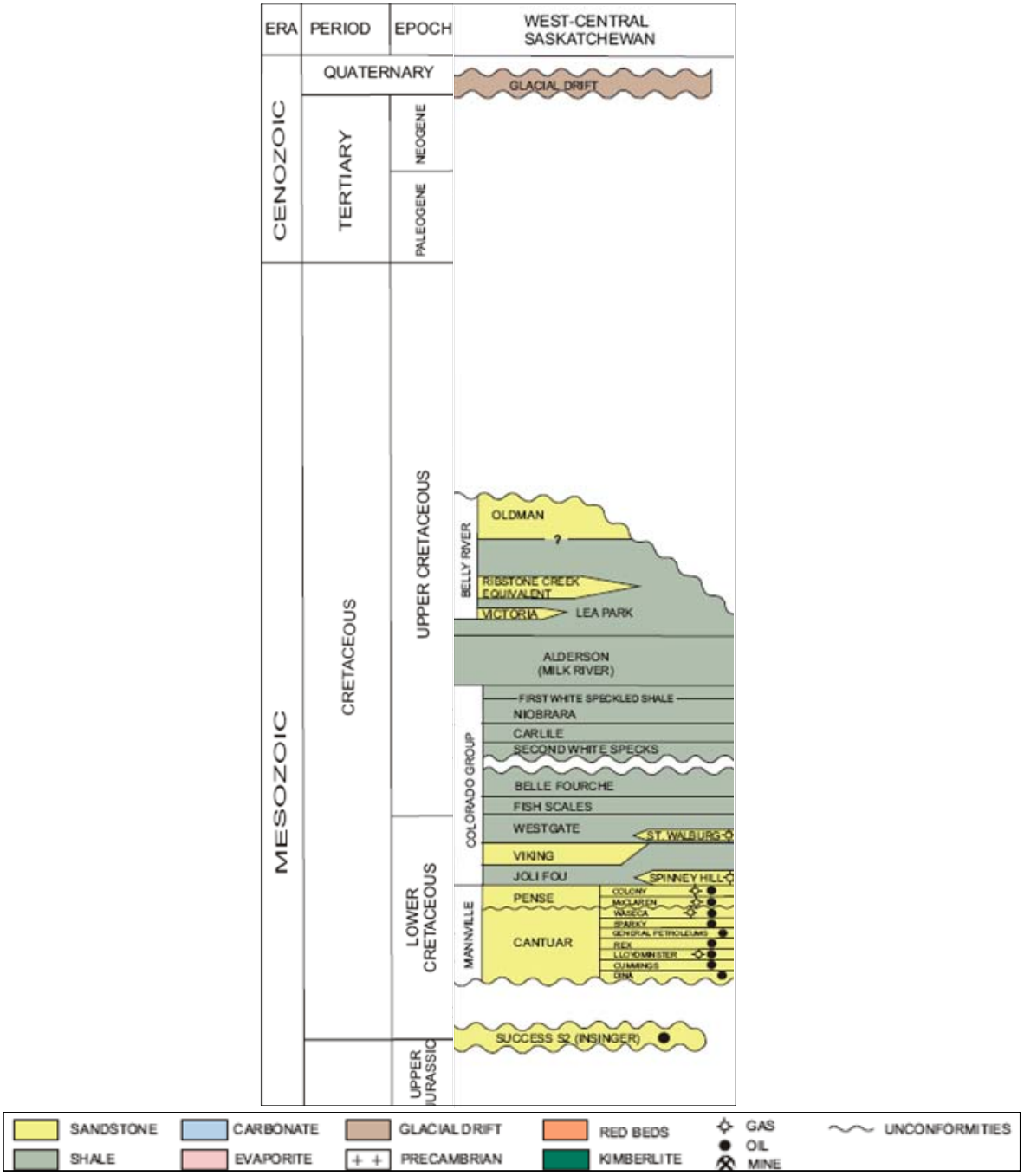

FIG. 2. Stratigraphic column for west central Saskatchewan (From Saskatchewan Industry and Resources, 2006).

The Sparky member conformably overlies the General Petroleum and it is capped by a regional coal marker. It is informally grouped into the middle Mannville, which is

dominated by sheet sandstone development, with narrow, channel sandstones and shales also present (Putnam, 1982). These units have been interpreted as a delta-front facies with associated tidal-flat, tidal-channel, and beach environments (Vigrass, 1977). The sheet sandstones in Sparky are commonly 6-9 m thick, and can be traced laterally for several tens of kilometers; however, they are commonly broken by thick ribbon-shaped deposits or sandstone pinchouts (Putnam, 1982). The Colony member consists of shales, siltstones, coals and sandstones. Deposition of this member occurred in an extensive complex of anastomosing channel sandstones, encased within siltstones, shales, coals and thin sheet sandstones (Putnam and Oliver, 1980). Three distinct facies have been interpreted within the Colony member: channel, crevasse splay and interchannel wetlands. Within the area of study, the reservoir rocks are represented by the channel facies.

The marine shales of the Joli Fou formation unconformably overlay the Colony member, representing the basal unit of the Colorado Group. This group is dominated by marine shales encasing generally thin but extensive sandstones, such as the Viking, Dunvegan and Cardium formations, which act as important petroleum reservoirs in other areas (Leckie et al., 1994). Within the Colorado Group, the First and Second White Speckled Shales, the Fish Scales Zone, and shale at the base of the Shaftesbury Formation are more radioactive than overlying and underlying shales, have high total organic carbon contents, and have considerable hydrocarbon generating potential. An interval such as the Second White Speckled Shale is potentially both a source and a reservoir rock for hydrocarbons (Mossop and Shetsen, 1994). Oil distribution and quality appear to be controlled by the hydrology of the reservoir body (Putnam, 1982).

GEOPHYSICAL DATA

The data available from the Manitou Lake oilfield includes a suite of logs from three well, as well as a 3D-3C survey in the area. A standard suite of logs, including Gamma-ray (GR), caliper (HCAL), spontaneous potential (SP), density (RHOB), neutron (NPHI) and density porosity (DPHI) for sandstone matrix, and shallow (RXOZ), medium (AHF30) and deep (AHF60) resistivity were available for each well. P-wave sonic is only available for well A11-17 and C07-16, while an S-wave sonic was also acquired in well A11-17.

A seismic survey was acquired for Calroc Energy Inc. by Kinetex Inc. in February 2005, consisting of twenty one south-north receiver lines and eighteen west-east source lines, with 200 m line spacing and 50 m station spacing (Lu et al., 2006). The exploration targets of this survey were sand channels within the Colony and Sparky members of the Mannville Group, which are currently producing oil in the area. Multicomponent data was acquired in an attempt to better delineate the reservoir sand channels.

ROCK PROPERTIES

Figure 3 shows the logs from well A11-17 over the interval of interest. Note the sharp decrease in the GR and SP logs at the top of the Colony sands, indicating the change from the shales of the Colorado Group to the predominantly sandy Mannville Group. At this interface the density log decreases, the P-wave shows almost no change and the S-wave velocity shows a very significant increase from 800 m/s in the shales to 1300 m/s in the

sands. High resistivity values in the Colony and Sparky members indicate hydrocarbons, while the cross-over between the density and neutron porosity logs in the Colony sands suggests gas. Several coal beds can be interpreted in the area, based on the lower density values, between 1.6 and 1.7 g/cm^3.

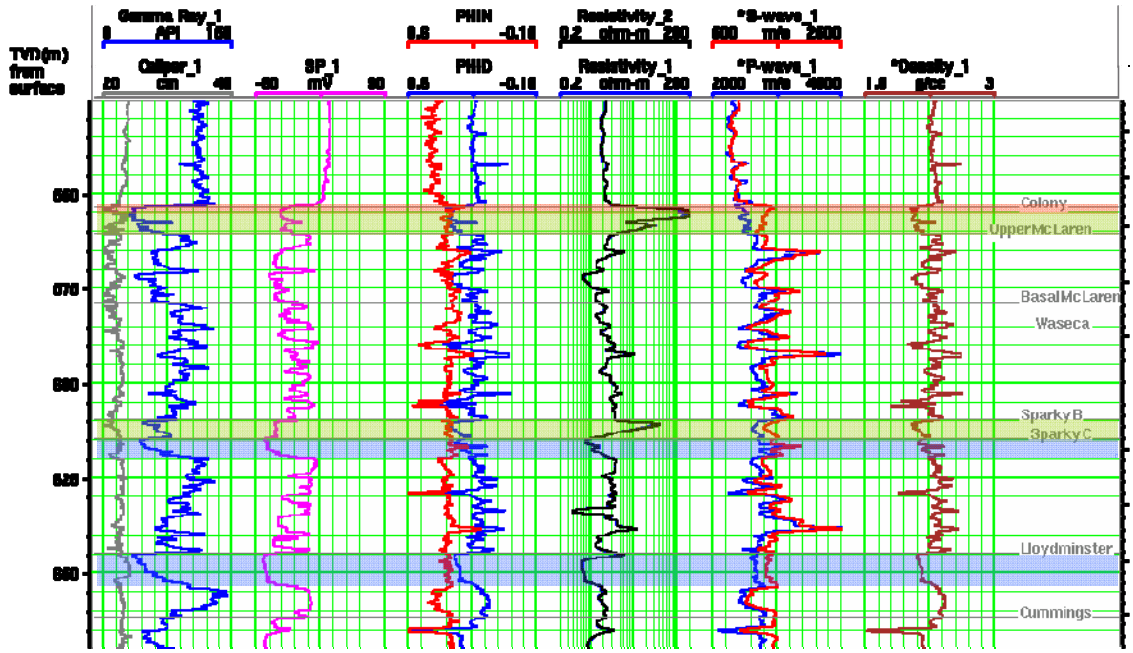

FIG. 3. Suite of logs for well A11-17. Gas is indicated by red highlight, oil by green and water by blue.

Note that the density and the velocity logs appear to be anticorrelated in some areas, especially at the top of the Mannville, where there is a significant decrease in the density and a slight increase in velocity. This increase in velocity is especially obvious in the case of the S-wave in the well A11-17 (See Figure 3). The area with higher GR values, between 300 and 400 m, is probably related to the more radioactive shales of the First and Second White Speckled formations, and the Fish Scales Zone, which have considerable hydrocarbon generating potential.

Figure 4 shows a series of crossplots from the logs in well A11-17. Note that over the complete depth interval of the logs density is not a good lithological indicator, as density values overlap for sands and shales, in a range between 2000 and 2400 Kg/m^3. P-wave velocity also shows overlap between sands and shales, with shales having a generally lower velocity than the sands. On the other hand, S-wave velocity shows very little overlap and appears to be the best lithological indicator, along with the Vp/Vs ratio, where sands have a ratio between 1.7 and 2.4, and shales between 2.4 and 4. However, within the target zone, density appears to be a good lithological indicator, with densities lower than 2250 kg/m^3 indicating sands, and higher values corresponding to shaly sands and shales (See Figure 5).

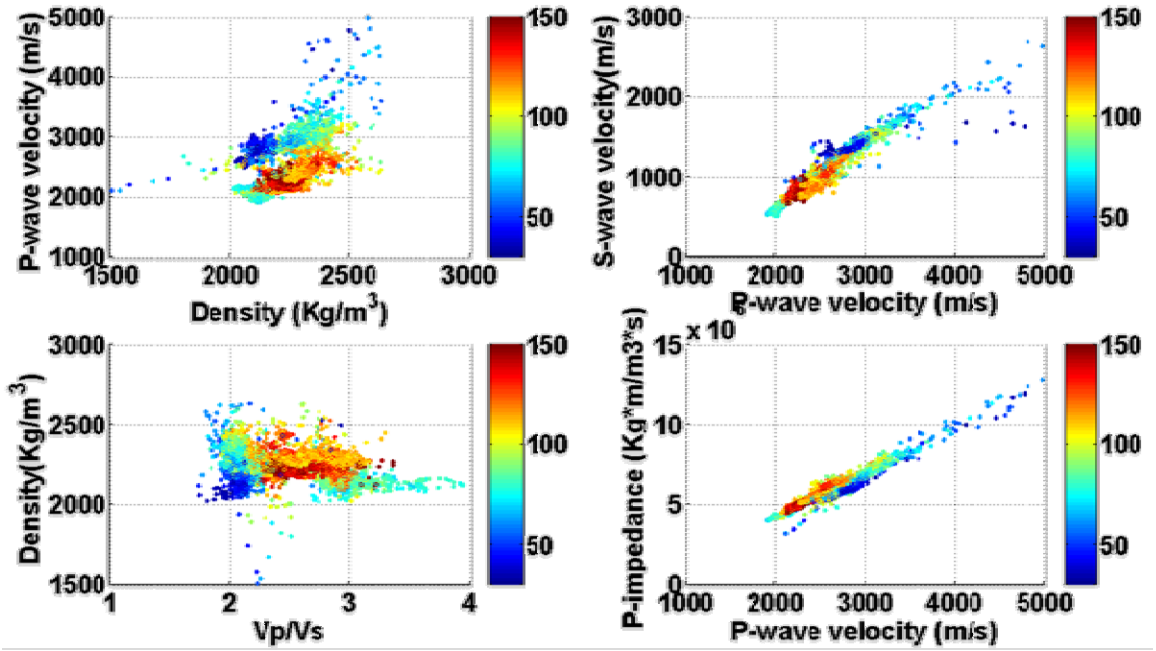

FIG. 4. Crossplots between different elastic properties for well A11-17. Colorbar indicates GR values.

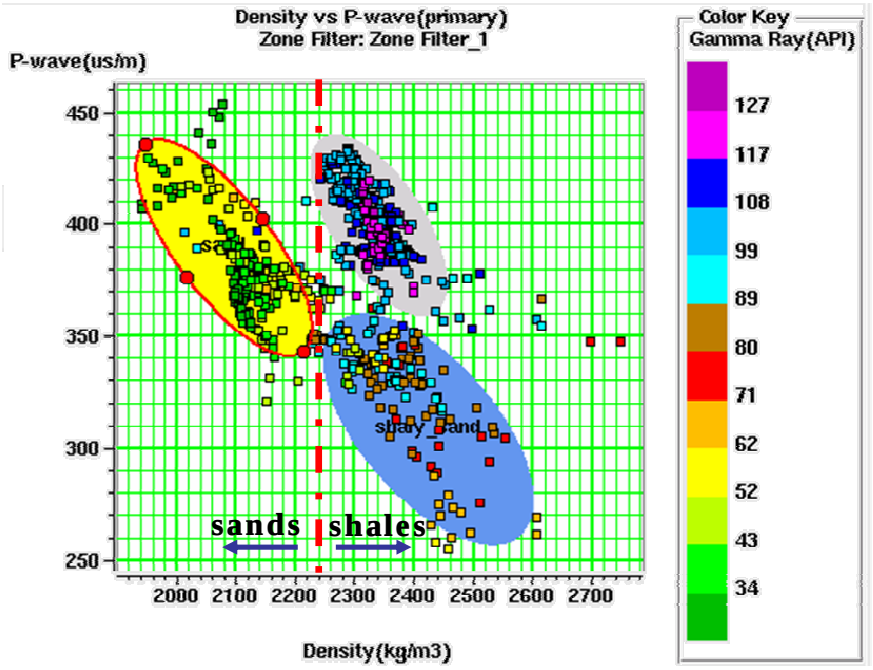

FIG. 5. P-wave velocity versus density crossplot for the interval between 500 and 600 m. Note that there appears to be a separation between sand and shaly sand at 2240 kg/m^3.

Across the whole depth interval, the Vp/Vs value appears to give the best differentiation with regards to lithology, with sands having a Vp/Vs value lower than 2.15 and shales having higher values. The sand reservoirs map within a very narrow

range of shear wave velocity, between 1300 and 1500 m/s. The mudrock line that relates P- and S-wave velocities fits very closely to the least-squares fit from the data.

Figure 6 shows density, P- and S-wave velocity crossplots for reservoir sands (GR <60 API units) with different saturating fluids, defined from the wireline logs. As expected, gas zones correspond to lower density and P-wave velocities. In general, oil zones have lower density and P-wave velocity than water zones, although there is still some overlap. Oil gravity in the area is very low, around 12° API, resulting in a density comparable to that of water, making it more difficult to differentiate oil and water zones using elastic properties.

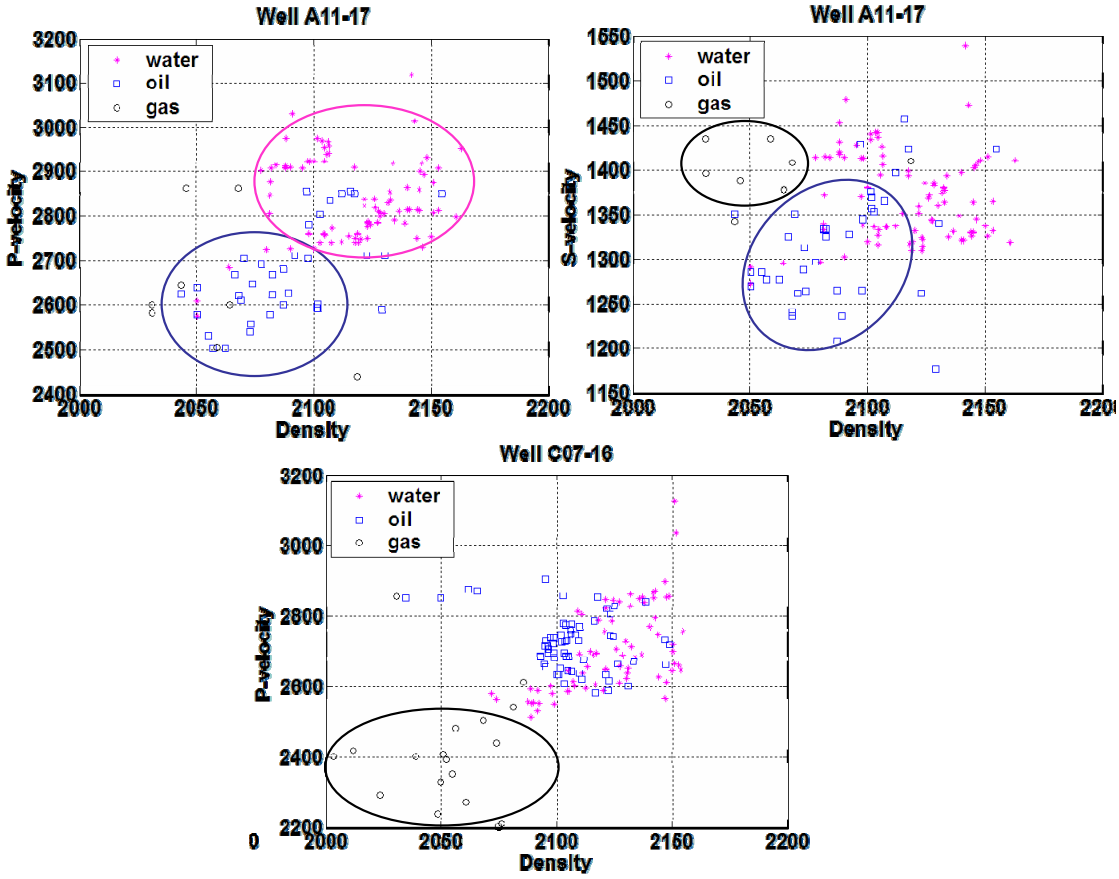

FIG. 6. Density, P-wave and S-wave velocity variations with saturating fluid based on log samples. Black circles correspond to gas, blue squares to oil and magenta stars to water.

Log response equation modelling

In this approach the rock is modeled as having four major components that contribute to the log reading (e.g. water, hydrocarbon, shale and matrix). The first term corresponds to the water contribution, the second to the hydrocarbon, the third is shale contribution and the final term is the contribution from the rock matrix (Figure 7).

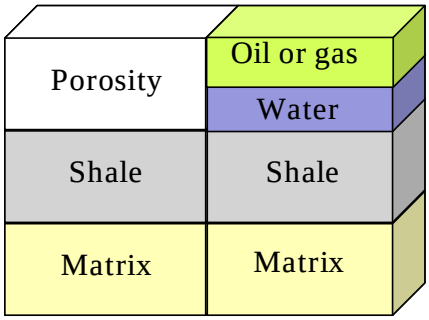

FIG. 7. Rock physics model for the log response equation.

Density, P-wave sonic and S-wave sonic logs can then be modeled using the following equation (Crain, 1986):

$$\log_{reading} = (\phi_e * S_w * \log_{water}) + (\phi_e * (1 - S_w) * \log_{hydro}) + (V_{sh} * \log_{shale}) + ((1 - V_{sh} - \phi_e) * \log_{matrix}), \quad (1)$$

where ϕ_e is the effective porosity corrected for shale volume, S_w is the water saturation, and *log* is the property value within each component.

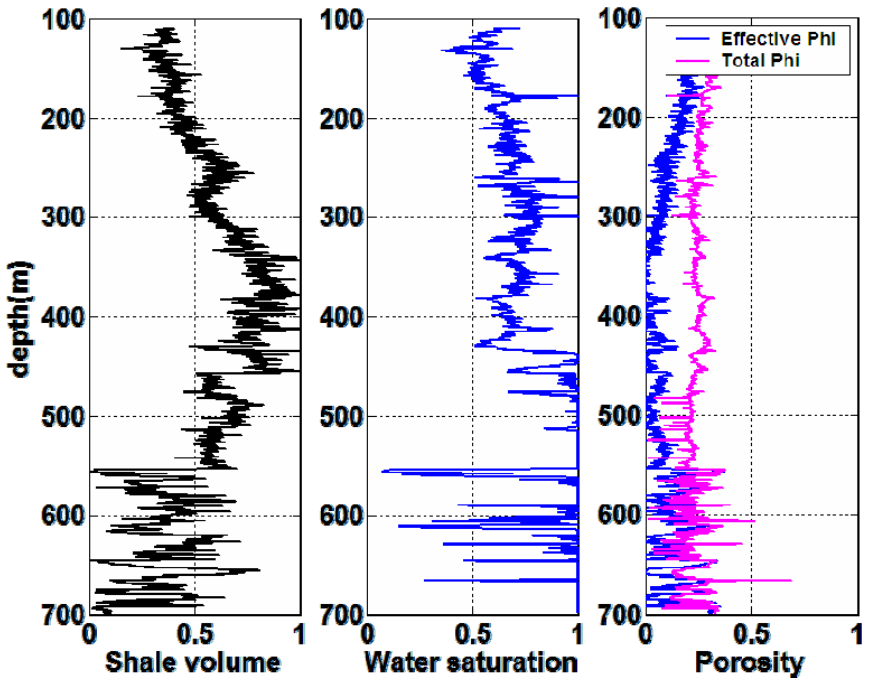

FIG. 8. Input logs for use in the log response equation (a) shale volume, (b) water saturation, and (c) porosity.

Shale volume was calculated from the GR log, effective porosity was calculated from the density-neutron crossplot method and corrected for shale volume (Figure 8). Log values for water, hydrocarbon and matrix were selected from the literature, based on the

known lithology and fluid properties (quartz matrix, and 12° API oil ≈ 0.98 g/cm^3). Shale values were selected directly from the logs, as they can have a wide range between different areas.

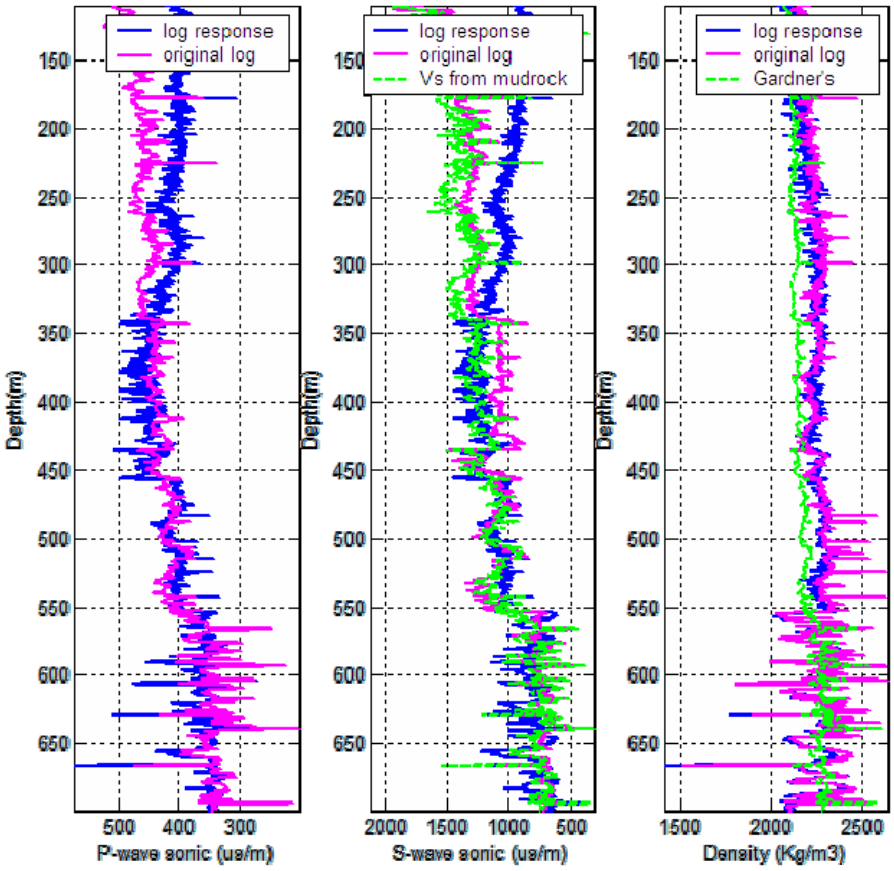

FIG. 9. Vp, Vs and density log values modeled using the log response equation.

Comparing results from the log response modeling and empirical relations (Figure 9), such as Gardner's and the mudrock line, we can note that the Vs estimates using the mudrock line are better, although they fail to reproduce the significant change in Vs at the top of the reservoir. If shear logs modeled from the mudrock line are used to generate synthetic seismograms, the response at the top of the reservoir will not tie with the seismic section.

This model results in very good density estimates; however, it fails to reproduce the P- and S-wave sonic logs adequately, especially in the shallower sections, as it does not incorporate the increase in matrix velocities with depth (or pressure or compaction). The pressure dependence of seismic velocities in unconsolidated sands is predicted by a power-law relationship, both by theoretical and empirical formulations. However, the exponents of the pressure differ significantly, with these differences being generally attributed to the non-spherical shape of real sand grains or to an increase in the average number of contacts per grain as the sample compacts with loading (Zimmer et al., 2007).

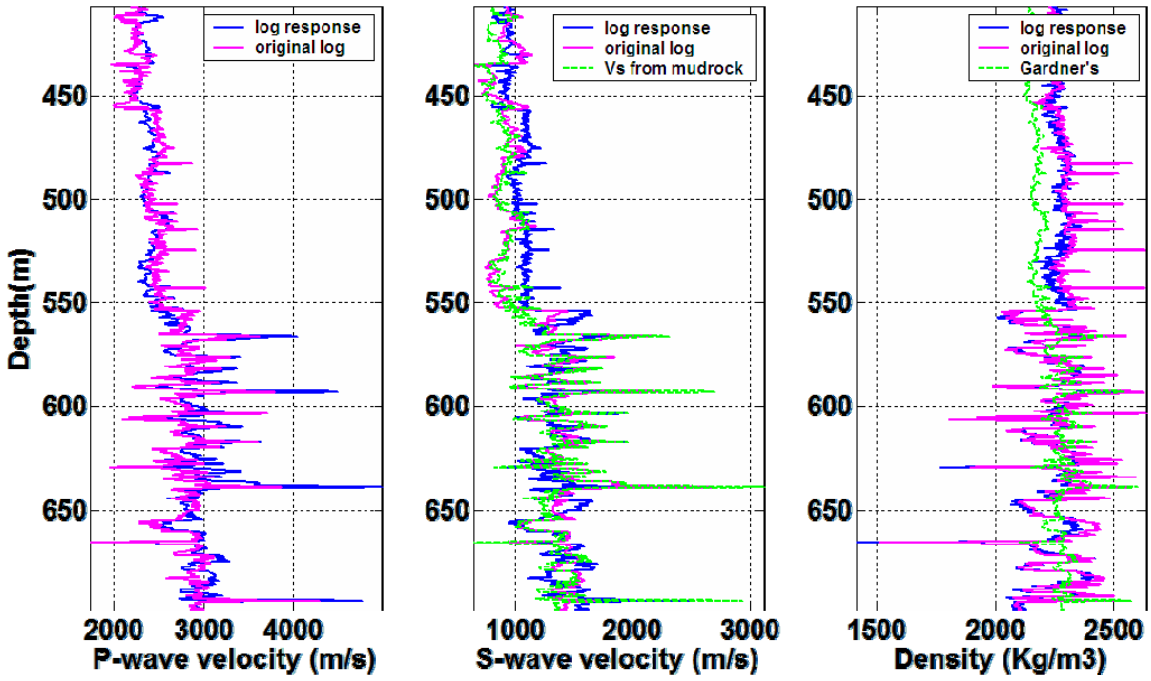

FIG. 10. Detail of modeled Vp, Vs and density logs in the interval of interest.

To evaluate the effects of pressure on the seismic velocities, it is necessary to determine the pressure gradient in the area. Lithostatic pressure was calculated from the weight of the overburden, integrating the density log with increasing depth, using the following equation:

$$P_{litho} = P_{atm} + g \sum \rho(z) \Delta z, \qquad (1),$$

where P_{atm} is atmospheric pressure at the surface, g is gravity acceleration and equal to 9.8 m/s^2, $\rho(z)$ is the density log value at each depth, and Δz is the depth interval. In normally pressured rocks, pore pressure is equal to the hydrostatic, which is the pressure due to the weight of the overlying fluid column. Finally, effective pressure is calculated by subtracting the pore pressure from the lithostatic pressure (Figure 11). Note that the effective pressure is almost equal to the hydrostatic pressure.

Zimmer et al (2007) measured compressional and shear wave velocities in a series of unconsolidated granular samples, including dry and water saturated natural sands, at pressures ranging from 0.1 to 20 MPa. They applied empirical fits to quantify the velocity-pressure behaviour of the samples, using a modified version of the Fam and Santamaria (1997) form as follows:

$$V_p = V_{p0} + OCR^k S \left(\frac{p\prime}{p_a}\right)^{n/2}, \qquad (2),$$

where p' is effective pressure and p_a is atmospheric pressure. The term OCR^k corrects for the effects of compaction or preconsolidation of the sample, where OCR is the

overconsolidation ratio, and k is a function of the plasticity index. The parameter k is usually assumed to be zero for clean sands, making the term OCR^k equal to 1.

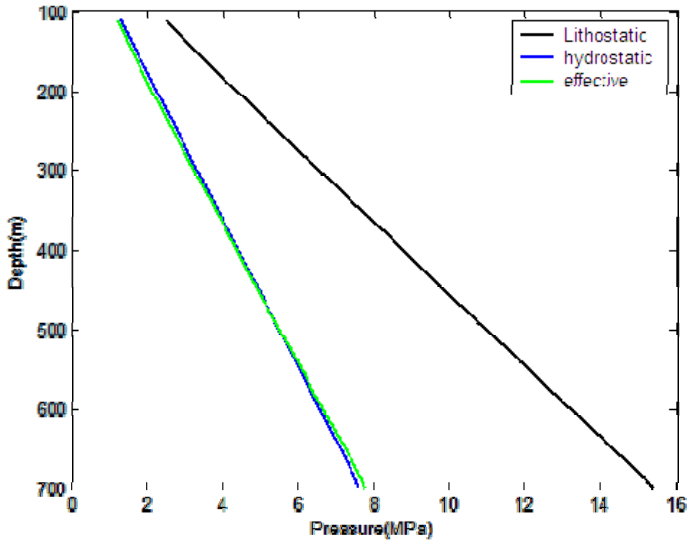

FIG. 11. Lithostatic (black), hydrostatic (blue) and effective (green) pressures calculated for well A11-17.

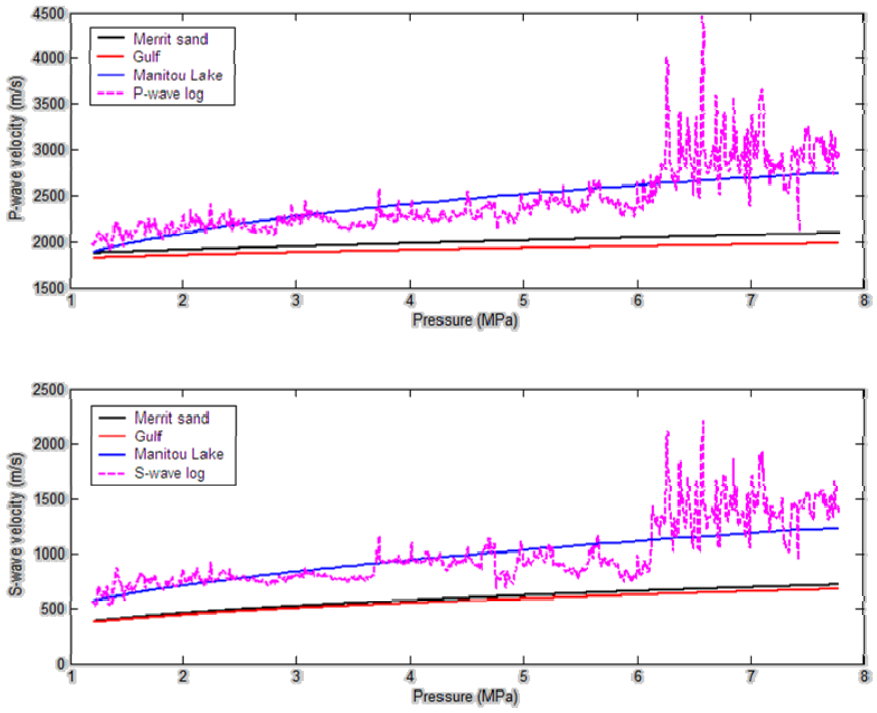

FIG. 12. P- and S- wave velocity variations with pressure calculated from equation 2, with fit parameters from the Merritt and Gulf of Mexico samples, and the local fit to velocity logs.

Equation 2 was fitted to the actual P- and S-wave velocity logs to compare with results for unconsolidated sands from the original study. Figure 12 shows the velocity

dependence with pressure using parameters for the Merritt and Gulf of Mexico sands and using the local fit parameters. Note the considerably higher velocity trend observed in the actual data. This difference can be attributed to consolidation of the sands within the area. However, applying these velocity-pressure trends within the log response modeling does not improve the modeled logs in the shallow section.

SYNTHETIC SEISMOGRAMS

PP and PS synthetic seismograms were generated for well A11-17 using Syngram program in Matlab (Figure 14 and 15). The PP synthetic was generated using a Ricker wavelet with a dominant frequency of 60 Hz, while the PS synthetic used a 40 Hz Ricker wavelet, to account for the lower bandwidth of PS data. It is interesting to note that the PP signature at the top of the Colony corresponds to a trough, while on the PS section it corresponds to a peak, showing the same type of behaviour at the top of the Sparky B (See Figure 13). This change in polarity between the PP and PS sections can significantly affect the registration process during the interpretation.

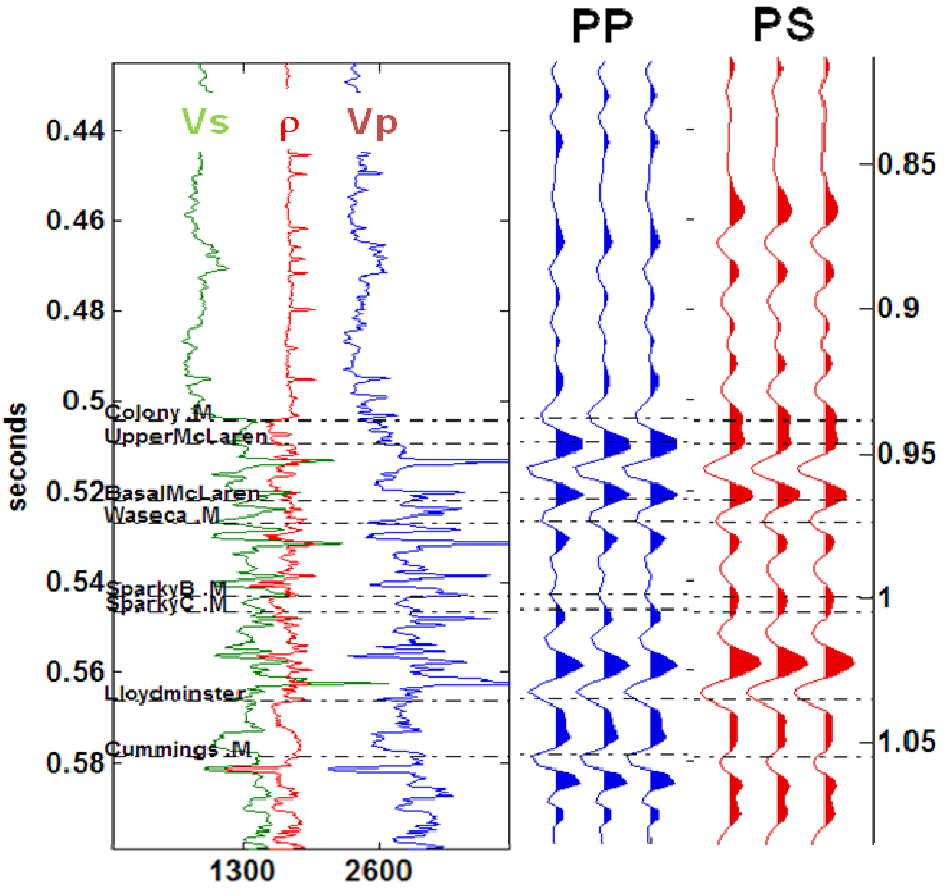

FIG. 13. Synthetic stacked PP (blue) and PS (red) traces for well A11-17.

Given the very different behaviour of the P- and S-wave velocities at the top of the sand channels, it is also expected that they will have different AVO character. The significant increase on the S-wave velocity at the top of the Colony suggests bright spots are expected in the PS section associated with sand intervals.

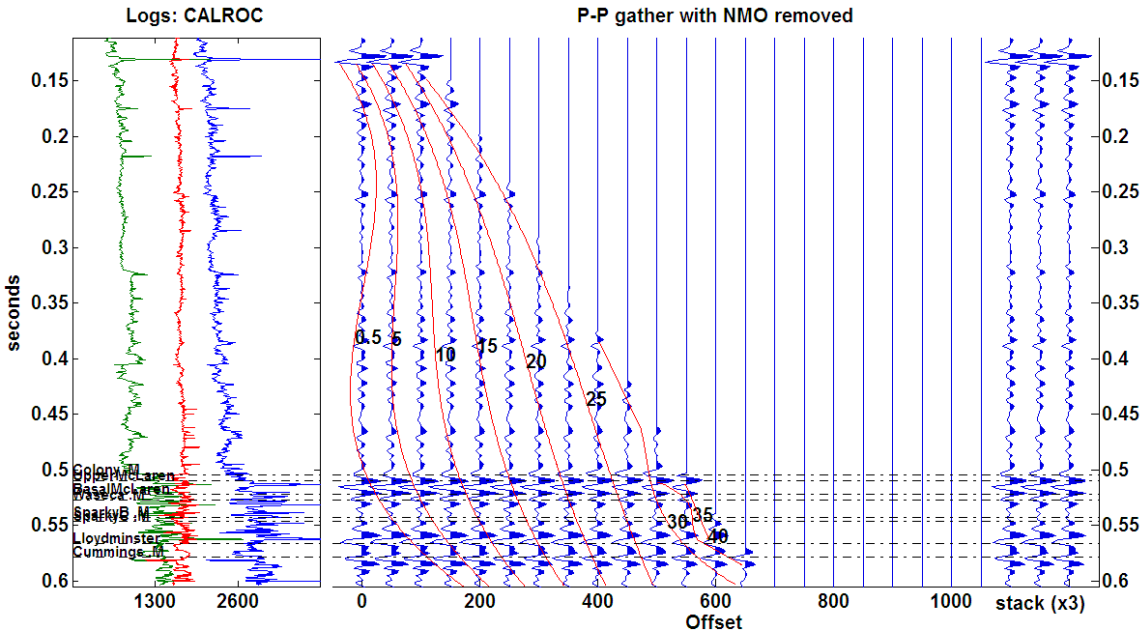

FIG. 14. Synthetic PP gather for well A11-17 with a 40 Hz Ricker wavelet, showing contours for the angle of incidence.

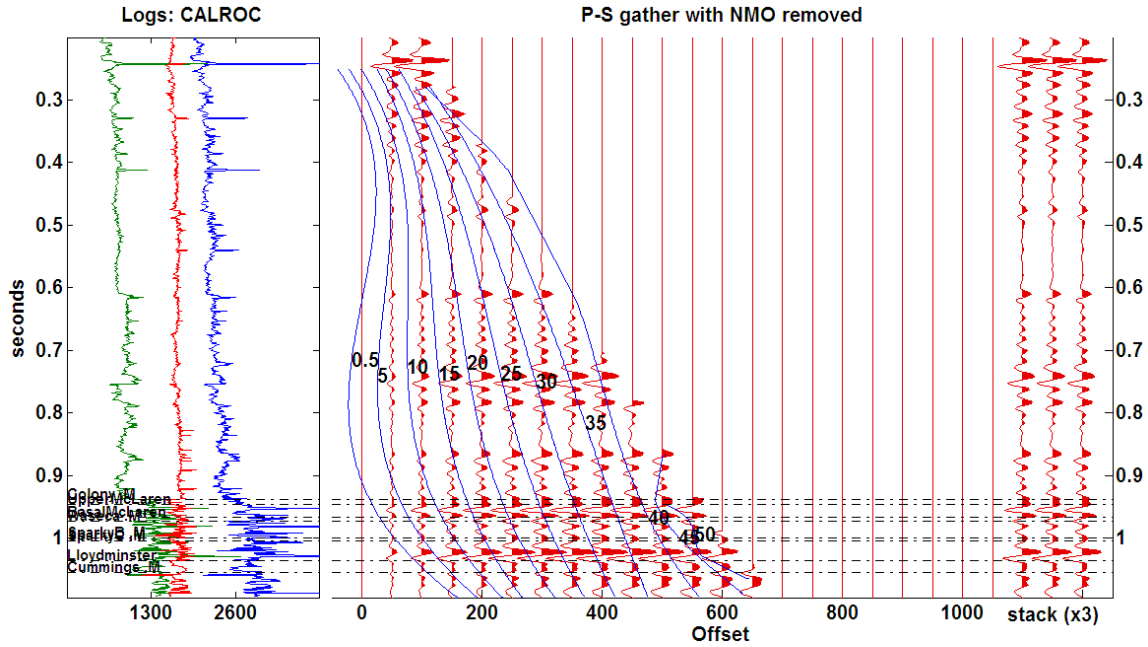

FIG. 15. Synthetic PS gather for well A11-17 with a 20 Hz Ricker wavelet, showing contours for angle of incidence.

IMPEDANCE INVERSION

A model based inversion using the generalized linear inversion algorithm (GLI) which attempts to modify the model until the resulting synthetic matches the seismic trace within some acceptable bounds, was used to estimate P-wave impedance from the PP seismic volume. This method is good when you have considerable knowledge about the geology and can create a reliable model.

An initial model for inversion was generated using P-impedance logs calculated at the two well locations with sonic logs available, with a high-cut filter of 10-15 Hz. The models used two picked horizons above and below the target zone to propagate the model away from the wells (Figure 16).

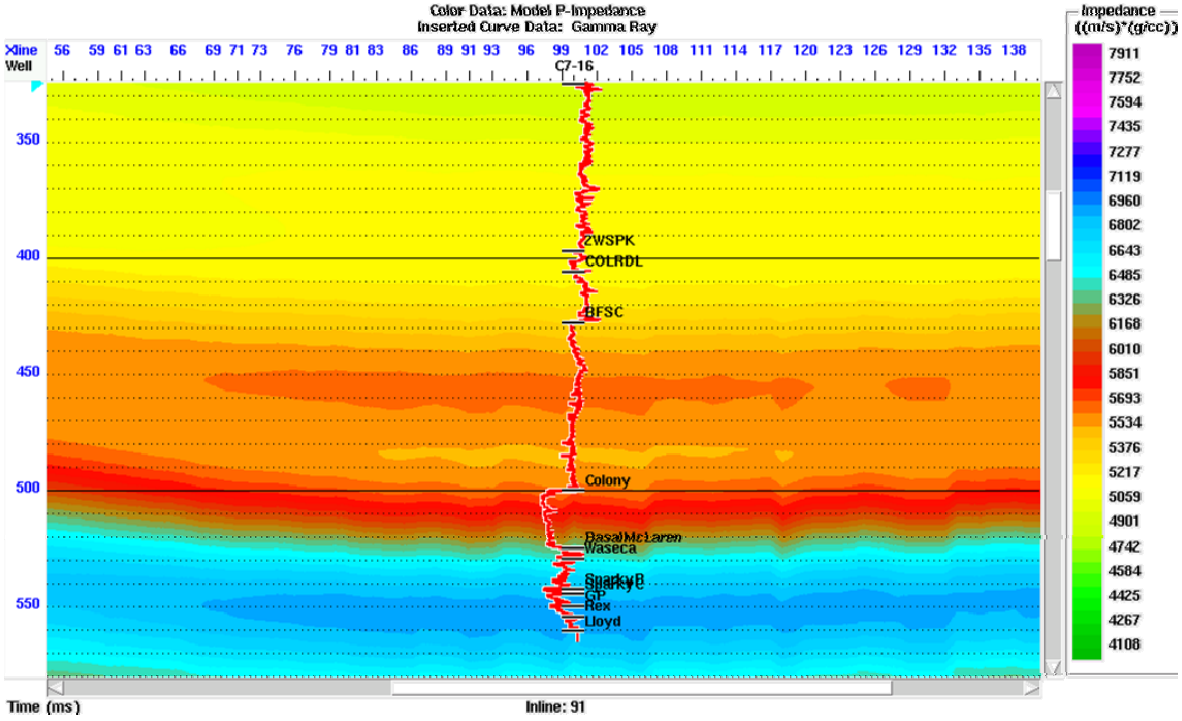

FIG. 16. Initial low frequency P-impedance model used in the model based inversion of the PP stacked volume.

A statistical wavelet was extracted from the PP seismic volume (Figure 17) at one of the well locations, between 400 and 650 ms, to be used in the model based inversion. A hard constrain of 100 % was used in the initial evaluation, indicating that impedance estimates are allowed to vary 100 % of their value with respect to the initial model. The inversion analysis performed at well C07-16 (Figure 18) shows very good agreement between the inverted and original impedance logs, and a high correlation between the seismic and the modeled synthetic.

The resulting impedance volume appears to give a good idea of the lateral extent of the channels at the Colony level, where the decrease in density is high enough to reflect on the impedance (Figure 19). However, the Sparky level is not imaged as well on the inverted volume, probably due to the smaller contrast with surrounding intervals.

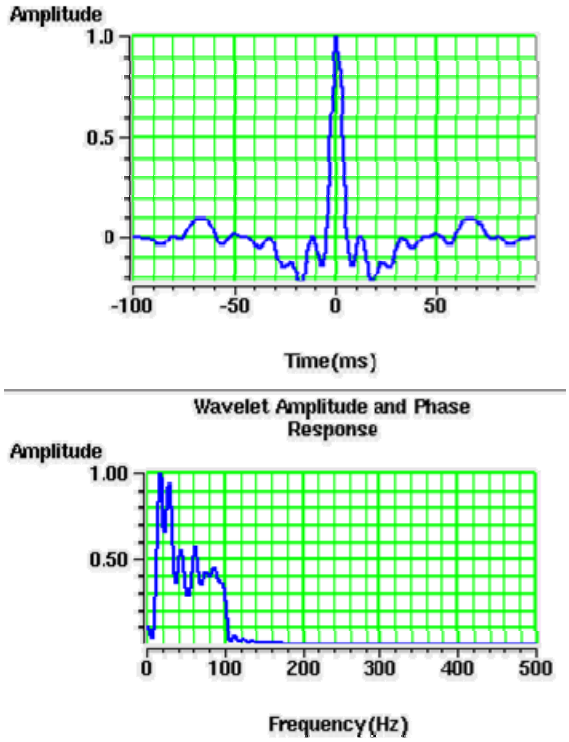

FIG. 17. Statistical wavelet extracted from the PP seismic volume.

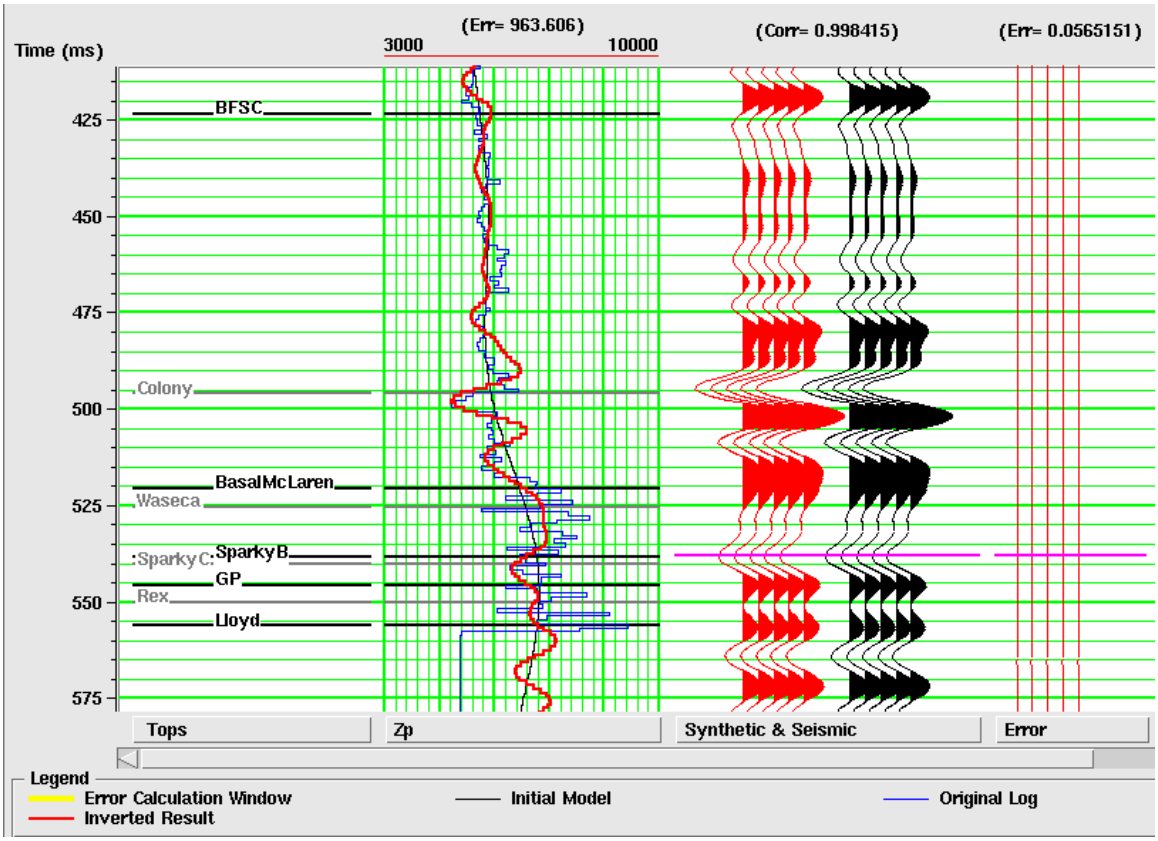

FIG. 18. Inversion analysis in well C07-16.

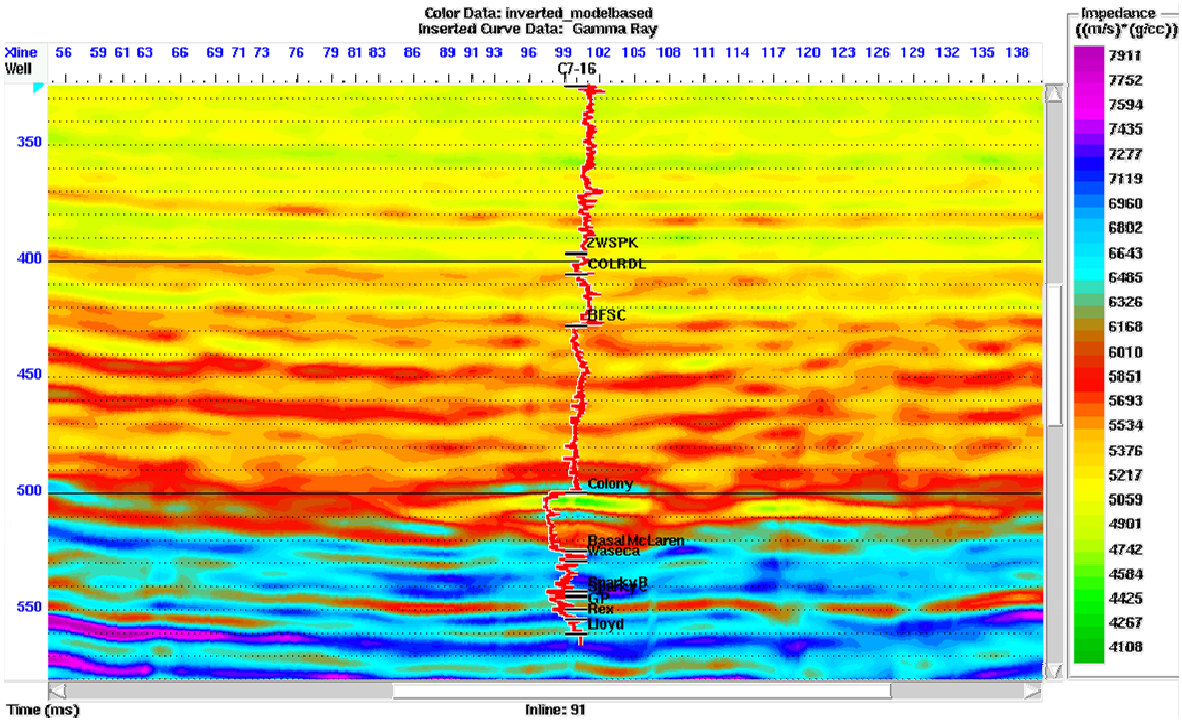

FIG. 19. P-impedance results from the model based inversion.

A band-limited impedance inversion using BLIMP software was performed on a single PS synthetic stacked trace. Impedance estimates using this method are very accurate as long as the low frequency model is close to the actual impedance. The original and modeled Vs logs were used to calculate density estimates from the inverted impedance. In this case, we can see that when using the correct log, the density estimates are reasonable. However, when using the modeled log, which deviated from the original log in some sections, the density estimates are completely distorted by these errors (Figure 20).

CONCLUSIONS

Shear-wave velocity is a very good lithological indicator in the area, showing a change of 500 m/s at the sand/shale interface, which results in significant changes in the PS section. Variations in density are more complex, as it is affected by the saturating fluid. Within the target zone, densities lower than 2250 kg/m^3 corresponds to clean sands, while shaly sands and shales have densities between 2250 and 2600 kg/m^3.

Post-stack inversion of the PP data show promise for delineating the channel. The decrease in density at the top of the Colony channel appears to be significant enough to be detectable through the P-impedance. However, these results do not seem to apply to the Sparky B member, where differences with surrounding intervals are more subtle.

ACKNOWLEDGEMENTS

We would like to thank Calroc Energy Inc. for providing this dataset to CREWES and Veritas Hampson-Russell (VHR) for the use of donated software (Geoview). We also would like to thank CREWES sponsors for their financial support.

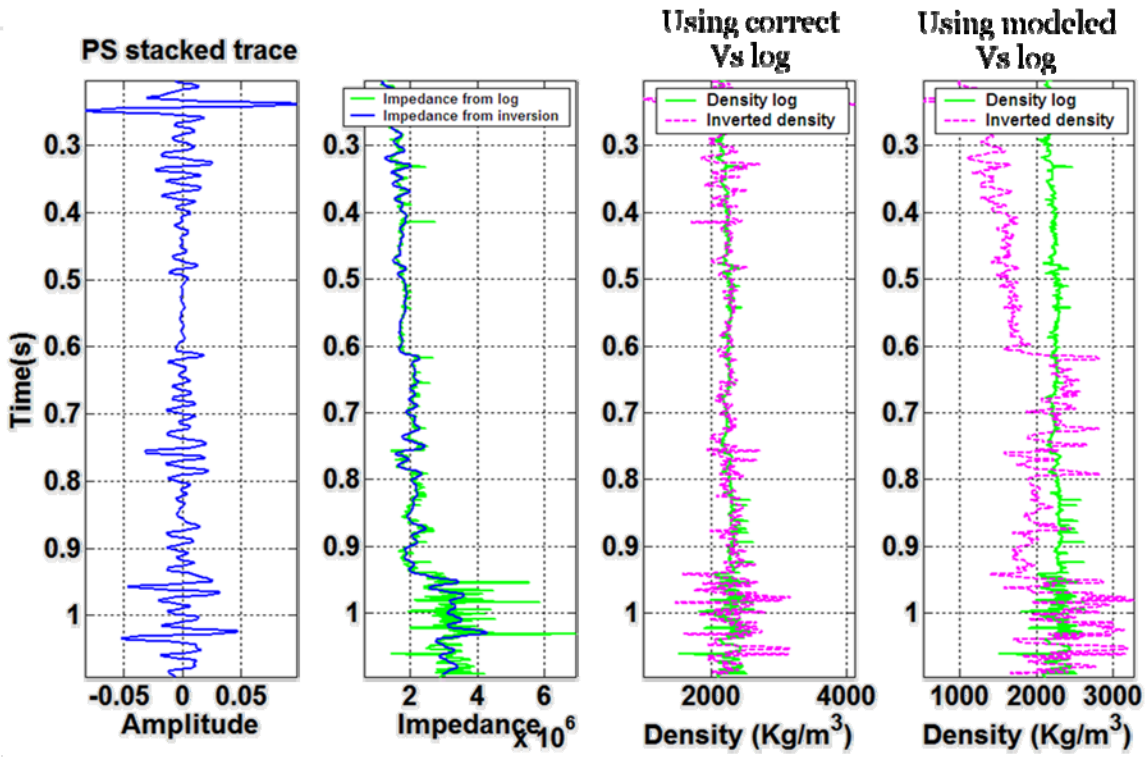

FIG. 20. Inversion of a single PS trace using BLIMP. Note instability of density results when using incorrect modeled logs.

REFERENCES

Castagna, J.P., M.L. Batzle, and T.K. Kan, 1993, Rock physics - The link between rock properties and AVO response in Castagna, J.P., and M. Backus, Offset dependent reflectivity, Theory and Practice of AVO analysis: SEG, 135-171.

Christopher, J. E., 1997, Evolution of the Lower Cretaceous Mannville Sedimentary Basin in Saskatchewan *in* Pemberton, S.G. and James, D.P.(eds.), Petroleum Geology of the Cretaceous Mannville Group, Western Canada, Can. Soc. Petrol. Geol. Memoir, **18**, 191-210

Crain, R., 1986, The Log Analysis Handbook: Pennwell.

Ferguson, R. J., and G.F. Margrave, 1996, A simple algorithm for band-limited impedance inversion: CREWES Research Report, **8**.

Gardner, G. H. F., L. W. Gardner, and A. R. Gregory, 1974, Formation velocity and density—the diagnostic basics for stratigraphic traps: Geophysics, **39**, 770–780.

Gray, F. D., P. Anderson, and J. Gunderson, 2006, Prediction of Shale Plugs between Wells in Heavy Oil Sands using Seismic Attributes: Natural Resource Research, **15**, no. 2, 102-109.

Putnam, P.E. and T. A. Oliver, 1980, Stratigraphic traps in channel sandstones in the Upper Mannville (Albian) and east-central Alberta. Bulletin of Canadian Petroleum Geology, **28**, 489-508.

Royle, A. J., 2002, Exploitation of an oil field using AVO and post-stack rock property analysis methods: 72nd Annual International Meeting, SEG, Expanded Abstracts, **21**, 289-292.

Van Koughnet, R. W., C. M. Skidmore, M. C. Kelly, and R. Lindsay, 2003, Prospecting with the density cube: The Leading Edge, **22**, 1038-1045.

Vigrass, L.W., 1977, Trapping of oil at intra-Mannville (Lower Cretaceous) disconformity in Lloydminster area, Alberta and Saskatchewan: American Association Petroleum Geologists Bulletin, **61**, 1010-1028.